Available online at www.sciencedirect.com
ScienceDirect
Journal of Molecular Catalysis A: Chemical 281 (2008) 207–213
JOURNAL OF MOLECULAR CATALYSIS A: CHEMICAL
www.elsevier.com/locate/molcata

Thermal decomposition study of silica-supported nickel catalyst synthesized by the ammonia method

Alfonso Loaiza-Gil *, Marlin Villarroel, José F. Balbuena, María A. Lacruz, Sergio Gonzalez-Cortés

Laboratorio de Cinética y Catálisis, Departamento de Química, Facultad de Ciencias, Universidad de Los Andes, Merida 5101, Venezuela

Available online 5 December 2007

Abstract

Silica-supported nickel catalyst synthesized by the ammonia method and their precursors treated and untreated with ammonia solution were studied by temperature-programmed reduction (TPR), scanning electron microscopy (SEM), and simultaneous thermogravimetry, differential scanning calorimetry and differential thermal analysis (TGA–DSC–DTA) carried out in nitrogen atmosphere (100 ml/min) at different heating rates (5, 10, 15 and 20 K/min). Temperature effect on the catalyst structural composition was studied by X-ray diffraction (XRD). The results indicated that synthesized catalyst shows mainly a higher temperature metal phase (973 K), constituted by a superposition of bi-dimensional sheets similar to nickel phyllosilicate, resulting from the strong metal–support interaction (SMSI) between nickel aqua ammine complex and silica surface. At high temperature, such a compound degrades to stable silica-supported nickel catalyst. Activation energies and kinetic parameters for each decomposition process were calculated by Kissinger's method. Enthalpy values were determined from differential scanning calorimetric profiles. The activity tests of such a catalyst to methane steam reforming indicated that deactivation process caused by carbon deposition was less pronounced than deactivation of a similar nickel content catalyst prepared by impregnation.

Keywords: Temperature-programmed reduction; Thermal studies; Nickel; Silica; Methane steam reforming

1. Introduction

The ammonia method has been used to synthesize silica-supported nickel and cobalt catalyst [1] in an effort to improve the metal dispersion and the attrition resistance and decreases the metal particle size and porous of the active phase. The method consists to contact the silica support with a metal nitrate solution to which ammonia solution was added. It was proposed [1,2], that ammonia attacks the silica support more or less strongly as revealed by the substantial increase of the specific surface area of that precursor [3,4]. Furthermore, metal aqua ammine complex ions formation like $[M(H_2O)_{6-n}(NH_3)_n]^{m+}$, (m = metal oxidation state, $n \leq 6$, coordination number), could be favored and its can reacts with the silica surface originating bi-dimensional metal-support compounds of ferromagnetic properties at low temperature [1]. The silica-supported nickel catalyst was obtained by reduction under hydrogen flow at 973 K. Previous studies performed on silica-supported iron and cobalt catalysts, by Fourier transformed infrared spectroscopy (FTIR), X-ray photoelectron spectroscopy (XPS), scanning electron microscopy associated with energy dispersive X-ray spectroscopy (SEM-EDS), X-ray diffraction (XRD) and thermal analysis (TG–DSC) suggested that iron and cobalt nitrates, at basic pH, give rise to metal aqua ammine complex ions formation that react with silica surface to form cobalt and iron phyllosilicates like $Co_3(OH)_4Si_2O_5$, $Co_3(OH)_2(Si_2O_5)_2$, $Fe_2(OH)_4Si_2O_5$ and $Fe_2(OH)_2(Si_2O_5)_2$. Their reduction has led to highly loaded Co/SiO_2 and Fe/SiO_2 [2,5,6]. Owing to the similarity of Ni^{2+} and Co^{2+} ions which both give rise to the same type of phyllosilicates [7] it was thought to prepare a silica-supported nickel catalyst using the same parameters employed for the preparation of silica-supported cobalt catalysts. As the first step, was considered more interesting to have a better understanding of the chemistry involved in the catalyst preparation which was likely similar to cobalt catalyst than focusing the attention on the preparation parameters influence, because of the large number of studies already done by Martin and co-workers focused to tuning the preparation parameters [1]. This

* Corresponding author. Tel.: +58 2742401371.
E-mail address: loaizag@ula.ve (A. Loaiza-Gil).

1381-1169/$ – see front matter © 2007 Elsevier B.V. All rights reserved.
doi:10.1016/j.molcata.2007.11.033

strategy requires the characterization of the precursor along the entire preparation route. Temperature-programmed reduction and scanning electron microscopy were employed to achieve information on the morphology and the number of metallic phases and thermogravimetry, differential scanning calorimetry and differential thermal analysis (TGA–DSC–DTA) were used to study the chemistry involved in the catalyst preparation. The last techniques demonstrated to be powerful tools to characterize the conformational changes induced by temperature in the sample under study, since they allow calculating the amount of decomposed sample, energy changes and the amount of heat involved in the decomposition reactions, besides the thermal properties of the sample.

Among the differential methods [8] for the study and determination of thermal decomposition kinetic parameters, the Kissinger's method has been the most used [9]. This method allows calculating the activation energy from calorimetric profiles obtained at different heating rates. The Kissinger equation can be expressed as

$$\ln\left(\frac{\beta}{T_m^2}\right) = -\frac{E_a}{RT_m} + C \quad (1)$$

where R is the universal constant of gases ($J\,mol^{-1}\,K^{-1}$), β is the heating rate ($K\,s^{-1}$), E_a is the activation energy ($J\,mol^{-1}$), T_m is the peak temperature (K) and C is a constant. The activation energy is obtained from the slope ($-E_a/R$), of the straight line obtained by plotting $\ln(\beta/T_m^2)$ against $1/T_m$. On the other hand, the peak shape of the resulting thermal analysis can be symmetrical or not. The peak symmetry is directly related with the reaction order of the chemical process. It was found [9] that when the reaction order $n = 1$, the peak has a symmetrical shape with similar areas on the right and on the left of the maximum inflection point (T_m). When the reaction order falls, the peak asymmetry increases. The left area of T_m is bigger than that on the right. Therefore, it is possible to use the peak shape as a variable to determine the reaction order from a differential thermal analysis (DTA). The shape index, S, is defined as the ratio between the slopes of the peak tangents at the inflection point. Furthermore, it was found that plotting S versus n^2, both parameters S and n are related according to the following equation:

$$S = 0.63n^2. \quad (2)$$

2. Materials and methods

2.1. Catalyst preparation

The silica-supported nickel catalyst was prepared according to a method similar to that described by Martin and co-workers [1]. The preparation of silica-supported 10% nickel catalysts was as follows: 2.81 g of $Ni(NO_3)_2{\cdot}6H_2O$ (98% purity, IQE) was added to 56 mL of distilled water at room temperature and vigorously stirred up to nickel salt dissolution. Nickel hydroxide was precipitated by addition of 2–3 drops of ammonia solution (28% NH_3, Fischer Scientific Company). A large excess of ammonia solution (56 mL) was added to dissolve the precipitate keeping the pH around 11–12. After 1 h stirring, 5 g of silica (aerosil 200 m^2/g specific surface area, Degussa) was added to the solution. The mixture was dried in an oven at 353 K for 48 h after 24 h stirring. The silica-supported nickel catalyst was obtained by reduction "in situ" under hydrogen flow (10 mL/min) at 1073 K. The reduction time lasted 24 h. In order to avoid unnecessary metal particles growing, the heating rate was set at 1 K/min.

2.2. Experimental methods

Thermogravimetry, differential scanning calorimetry and differential thermal analysis were carried out simultaneously on a Thermal Analyzer TA Instruments, model SDT Q600 (1773 K) under nitrogen flow (100 mL/min) using an average weight of 7.3 mg of sample and 5, 10, 15 and 20 K/min heating rate. XRD measurements were performed in a powder diffractometer Phillips PW1050/25 equipped with a Cu Kα ($\lambda = 1.5406$ Å) radiation source. The XRD data were taking at 2θ angular range, step size of 0.002° and 10 s count time.

Temperature-programmed reduction profiles (TPR) were performed on a Micromeritics TPR/TPD 2900 from room temperature to 1073 K at 10 K/min heating rate under 50 mL of 10% hydrogen in argon. Samples of 150 mg were pretreated in air before the TPR measurements. Micrographs were performed on a scanning electron microscope Hitachi, S-2500.

Catalytic performance of silica-supported nickel catalyst for methane steam reforming was tested in a continuous, fixed-bed tubular reactor described previously [13]. A controlled heater ensured a uniform bed temperature monitored by a thermocouple placed in the reactor center. Carbon monoxide, carbon dioxide and light hydrocarbons were analyzed by online gas chromatography (Hewlett Packard 6890 Plus) equipped with a thermal conductivity detector and a Porapak Q column (10 ft. × 1/8 in., 80/100 mesh). 0.4 g of the catalyst was reduced "in situ" under 10 mL/min of hydrogen flow from room temperature to 1073 K, at 1 K/min heating rate for 24 h. The reaction was performed at 973 K, atmospheric pressure and 500 h^{-1} gas hour space velocity (G.S.H.V.) using wet methane ($CH_4 + H_2O$). After run the gas feed was closed and the reaction temperature was sharply decreased to room temperature.

3. Results and discussion

Simultaneous thermal analyses TGA–DSC and DTA on hexahydrate nickel nitrate carried out between room temperature and 670 K and 15 K/min heating rate, are shown in Figs. 1 and 2 respectively. Fresh nickel salt precursor show five endothermic peaks and 73.2% total mass lost due to water dehydration and thermal decomposition of nitrates giving rise nickel oxide formation (II). The residual weight of 26.8% suggests that molecular weight of nickel salt precursor was quite similar to that reported. The molecular weight of thermal decomposed sample was calculated by the following equation:

$$\text{residue}(\%) = \frac{\text{M.W.}_{\text{NiO}}}{\text{M.W.}_{\text{initial compound}}} \times 100 \quad (3)$$

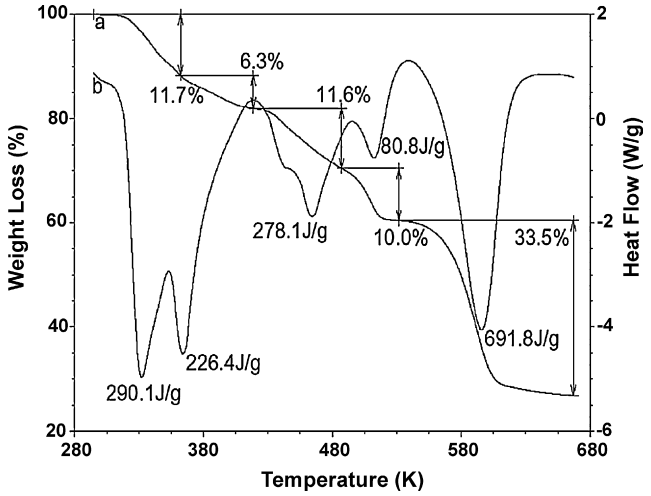

Fig. 1. Simultaneous (a) TGA and (b) DSC profiles (nitrogen flow, 100 mL/min) of commercial $Ni(NO_3)_2{\cdot}6H_2O$ at 15 K/min, heating rate.

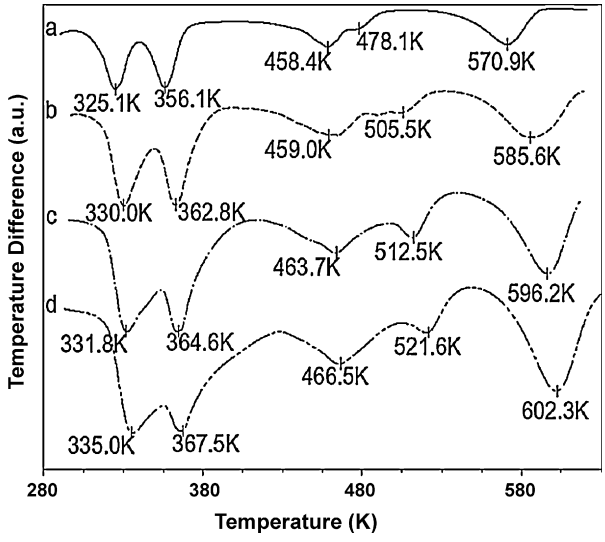

Fig. 2. DTA profiles of commercial $Ni(NO_3)_2{\cdot}6H_2O$ (nitrogen flow, 100 mL/min) at (a) 5 K/min, (b) 10 K/min, (c) 15 K/min and (d) 20 K/min heating rate.

The small weight difference (0.4%) found on commercial nickel nitrate hexahydrate could be due to hydration water lost by salt manipulation [10,11].

The first two decomposition steps occur along 331–364 K and were assigned to hydration water lost. The dehydration temperature difference was found to be dependent on the existence on nitrates groups which several water bond types [10–14]. The following two decomposition steps occur around 463–512 K and are harder to explain. It was proposed [13,14] that these two steps correspond to water and NO_x losses and to the formation of intermediate compounds type nickel hydroxynitrates $Ni_2(NO_3)_2(OH)_2$ and nickel oxynitrates $NiO.NiONO_3$. The last step could be assigned to NO_x and O_2 lost from the intermediate compounds originating stable nickel oxide. The enthalpy values of 290.1, 226.4 and 278.1 kJ/mol obtained for the first three decomposition steps (Table 1) suggests that water molecules with different bonding type were liberated. These results agreed very well with the decomposition pattern of moisturized transition metal nitrates reported by Malecki et al. [13] and Zivkovic et al. [14].

Two roles were proposed [1] for the ammonia solution: the first one was the functionalization of the silica support according to the following reaction:

$$\text{Si–OH} + \text{NH}_3 \rightarrow \text{SiO}^-\text{NH}_4^+ \quad (4)$$

The second one was the formation of nickel aqua ammine ions, $[Ni(H_2O)_{6-n}(NH_3)_n]^{2+}$ which exchange with surface NH_4^+ ions. Taking account of two OH^- groups for the electric charge balance of nickel aqua ammine ion, in solid state, the molecular weight of nickel salt treated with ammonia solution was expected to be between 200 g/mol ($n=0$) and 194 g/mol ($n=6$).

The TGA–DSC and DTA experiments on nickel salt treated with ammonia solution (dried by solvent evaporation) can lighting the second approach and are shown in Figs. 3 and 4 respectively. The thermogravimetric profile show in this case a decomposition pattern on three steps and 65.5% total mass lost (35.5% residue). The calculated molecular weight (Eq. (3)) of 217 g/mol resulted to be superior to the expected value. The difference between the expected and calculated molecular weight could be caused by an incomplete sample dried. The DSC profile of this sample shows two endothermic peaks with mini-

Table 1
Calculated kinetic decomposition parameters of synthesized silica-supported nickel catalyst and their precursor treated and untreated with ammonia solution

Sample	Weight losses	ΔH (KJ/mol)	S	n	E_a (kJ/mol)	ln A	κ (s^{-1})
Ni phyllosilicate	1	292.1	1.1	1.3	48.9 ± 0.6	21.0	15.6
	2	243.3	0.4	0.8	91 ± 3.0	24.4	12.8
$Ni(NO_3)_2{\cdot}6H_2O$ (ammonia treated)	1	116.1	1.3	1.4	57 ± 1.0	24.4	18.5
	2	308.8	2.6	2.0	151 ± 1.8	48.2	30.2
	3	−505.1[a], 254.6	2.9	2.1	220 ± 3.0	49.1	21.9
Untreated $Ni(NO_3)_2{\cdot}6H_2O$	1	290.1	2.3	1.9	125 ± 1.2	49.2	37.9
	2	226.4	0.9	1.2	127 ± 1.2	45.7	33.0
	3	278.1	0.8	1.1	236 ± 8.0	64.9	37.7
	4	80.81	0.4	0.7	57 ± 0.8	15.6	8.0
	5	691.8	0.6	1.0	115 ± 3.0	25.9	11.4

[a] Exothermic process.

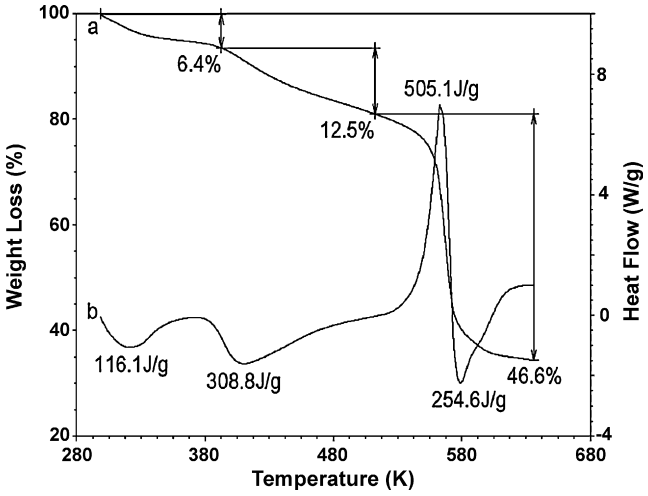

Fig. 3. Simultaneous (a) TGA and (b) DSC profiles (nitrogen flow, 100 mL/min) of nickel nitrate hexahydrate treated with ammonia solution at 15 K/min heating rate.

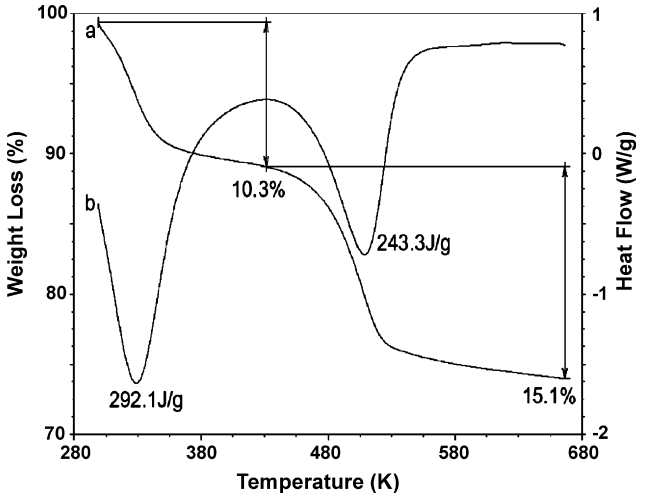

Fig. 5. Simultaneous (a) TGA and (b) DSC (nitrogen flow, 100 mL/min) of silica-supported nickel catalyst carried out at 15 K/min, heating rate.

mum at 325 K ($\Delta H = 116.1$ kJ/mol) and 399 K ($\Delta H = 308.8$ J/g) suggesting a loss of physisorbed and structural water respectively in that order. The third DSC peak was exothermic suggesting a great structural rearrangement before the occurrence of the last endothermic decomposition that give rise to nickel oxide formation. Such a result indicated that the reaction between ammonia and nickel nitrate hexahydrate to form nickel aqua ammine complex ions has a good chance to occur.

The next step in this work was to check out the chemical composition of the synthesized silica-supported nickel catalyst before the reduction process. The thermal analysis TGA–DSC and DTA of this catalyst is shown in Figs. 5 and 6 respectively. The TG profile show that 25.4% total mass lost occurs in two steps giving rise NiO/SiO_2 catalyst (10%Ni). The result suggests that three water or ammonia molecules were lost in the first step and four in the second without any further structural rearrangement observed. However, the calculated activation energies (Table 1) of 48.92 and 90.92 KJ/mol for the first and second steps in that order suggest that in addition of water and/or ammonia lost, structural rearrangement, bonds broken and/or formation occurs. On the other hand, comparing the calculated activation energies values of synthesized catalyst and treated nickel salt, it was found that the activation energy on the second decomposition step of synthesized catalyst does not correspond with any decomposition step of treated nickel salt as confirmed by the different values of the calculated reaction order n (Table 1), suggesting that silica and nickel aqua ammine complex ions reacts between them originating a new compound that in our case could be corresponding to nickel phyllosilicate hydrate. The weight lost observed for the synthesized catalyst (Fig. 5) suggested that the decomposition process

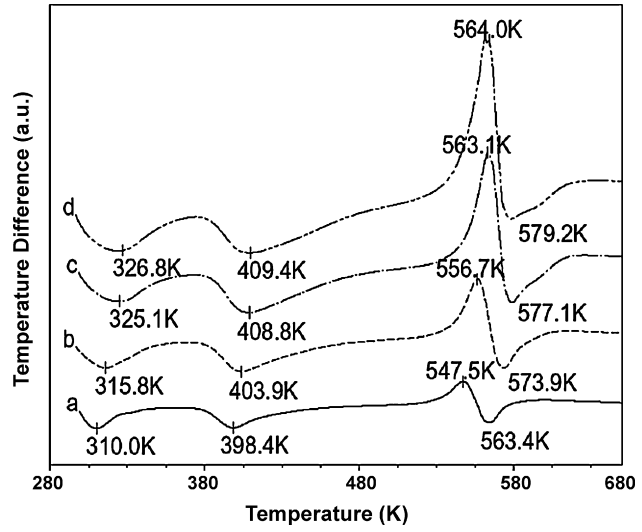

Fig. 4. DTA profiles (nitrogen flow, 100 mL/min) of nickel nitrate hexahydrate treated with ammonia solution at (a) 5 K/min, (b) 10 K/min, (c) 15 K/min and (d) 20 K/min heating rate.

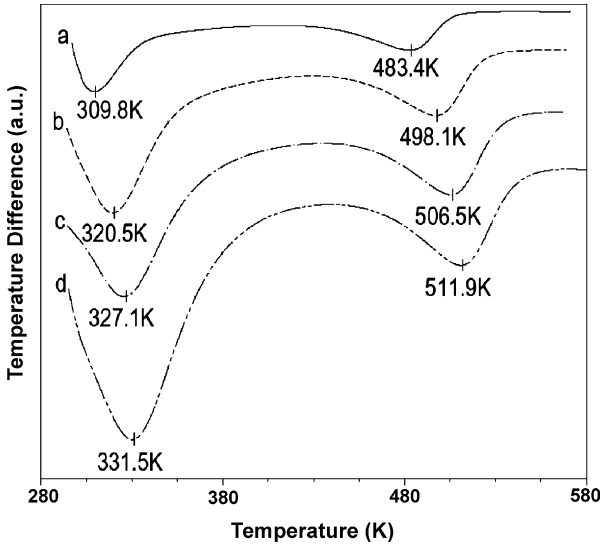

Fig. 6. DTA profiles (nitrogen flow, 100 mL/min) of silica-supported nickel catalyst at (a) 5 K/min, (b) 10 K/min, (c) 15 K/min and (d) 20 K/min heating rate.

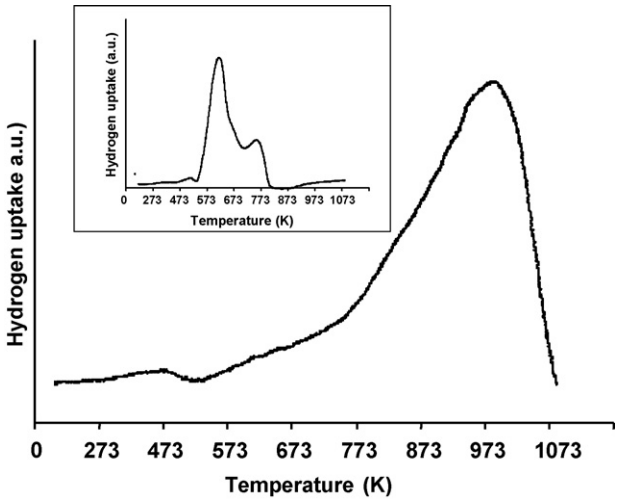

Fig. 7. Temperature-programmed reduction profile of silica-supported nickel catalyst synthesized by the ammonia method. On the left corner (up): temperature-programmed reduction profile of silica-supported nickel catalyst synthesized by impregnation.

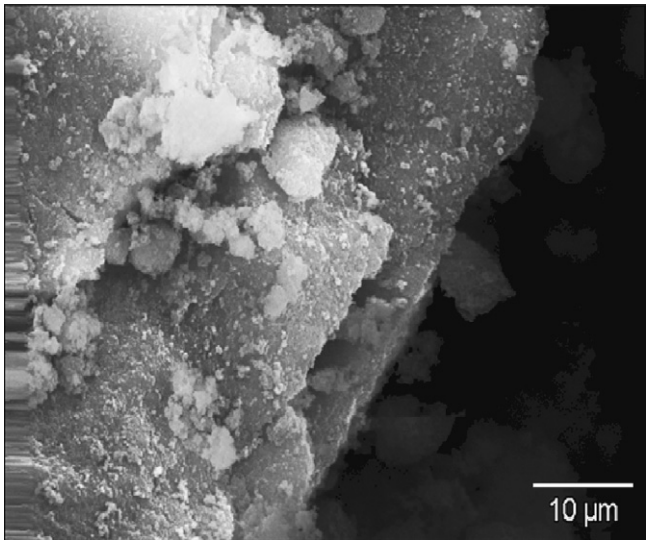

Fig. 8. SEM micrograph of silica-supported nickel catalyst synthesized by the ammonia method. The sample was dried at 423 K.

of the synthesized catalyst occur according to the following reactions:

$$Ni_3(OH)_2(Si_2O_5)_2{\cdot}6H_2O \rightarrow Ni_3(OH)_2(Si_2O_5)_2{\cdot}3H_2O + 3H_2O \quad (5)$$

$$Ni_3(OH)_2(Si_2O_5)_2{\cdot}3H_2O \rightarrow 3NiO + 4SiO_2 + 4H_2O \quad (6)$$

Such a result agreed quite well with that obtained by Martin and co-workers [1] and suggests that the use of ammonia method favor strong metal–support interaction (SMSI) formation. In order to verify the chemical and structural composition of the catalyst, further experiments of temperature-programmed reduction and scanning electron microscopy were performed. Temperature-programmed reduction profiles of silica-supported nickel catalyst synthesized by the ammonia method and by impregnation are shown in Fig. 7. It was observed that the catalyst synthesized by the ammonia method show mainly a high temperature metal phase with maximum around 973 K corresponding to SMSI and a small contribution of NiO at 473 K. Instead, silica-supported nickel catalyst synthesized by impregnation show two reduction peaks at 588 and 753 K corresponding to NiO free and weakly associated to the support [15,16]. A micrograph of silica-supported nickel catalyst, dried at 423 K was shown in Fig. 8. It was observed a structure constituted by superimposed sheets similar to nickel phyllosilicate in agreement to TGA–DSC and TPR results.

Fig. 9 shows the X-ray diffraction patterns of silica treated and untreated with ammonia solution and silica support nickel catalyst. It was observed for all of three patterns a shoulder around $2\theta = 23^\circ$ characteristic of amorphous substances. Besides, the diffraction pattern of silica support nickel catalyst shows two small shoulders around 37° and 63° probably corresponding to NiO species from the lower temperature metal phase (473 K) determined by TPR. A similar diffraction pattern was found for cobalt phyllosilicate catalyst [17]. Fig. 10 compares the silica support nickel catalyst diffraction patterns, fresh and after being calcinated at 373, 473 and 773 K. It was observed basically the same diffraction pattern as the temperature increases suggesting that catalyst chemical structure was thermally stable up to 773 K. This last result agreed very well with the TPR results that indicated that 973 K temperature or more was necessary to collapse the catalyst structure.

Preliminary catalytic test of methane steam reforming performed on the silica-supported nickel catalyst synthesized by the ammonia method and by impregnation are shown in Figs. 11 and 12. Typical deactivation curves, probably caused by inactive carbon deposition were observed for both catalysts.

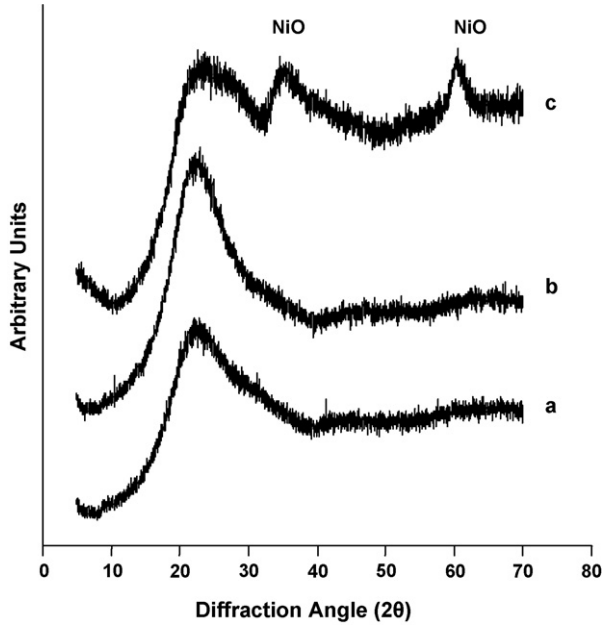

Fig. 9. XRD of (a) commercial silica (200 m^2/g), (b) commercial silica (200 m^2/g) treated with ammonia solution and (c) silica-supported nickel catalyst dried at 353 K.

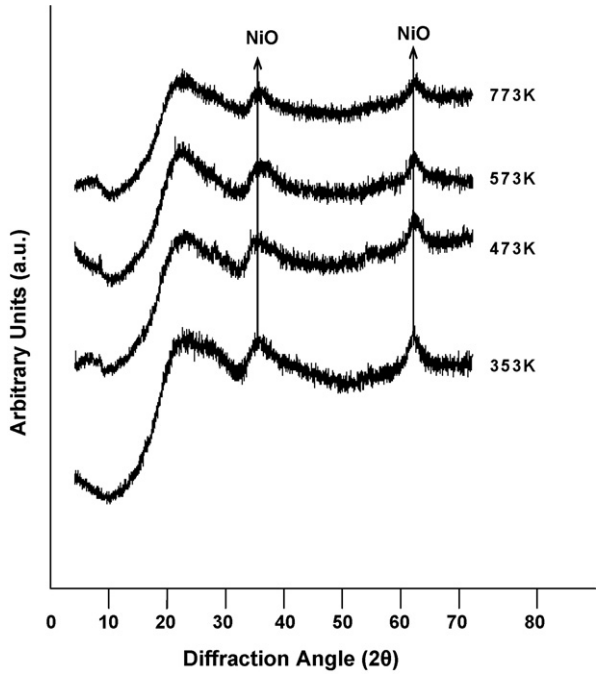

Fig. 10. XRD of silica-supported nickel catalysts dried at several temperatures.

The conversion of methane versus time on the catalysts synthesized by the ammonia method is displayed in Fig. 11(a). It was observed a dramatically decreases of the conversion from 100 to 62% on the first 50 min followed by a further conversion decrease after a period of 600 min of slowly conversion decreases. After that the methane conversion was observed to be constant around to 50% for the rest of the reaction time tested. The selectivity to hydrogen was observed (Fig. 11(b)) to decrease from 100 to 92% on the reaction time. As the same way the selectivity to carbon monoxide was observed to increases up to 8%. No carbon dioxide was detected. The performance of this catalyst to the steam reforming was compared with a similar catalyst synthesized by impregnation. In Fig. 12(a), it was observed that, conversion decreases on the first 500 min from 100 to 56%. After that the conversion decreases with a different deactivation rate arriving to 35% at the end of the test. The selectivity to hydrogen decreased from 100 to 85% on the entire reaction time while the selectivity to carbon monoxide was progressively increasing. Also in this case, no carbon dioxide was detected.

The performance of the catalyst synthesized by the ammonia method was better than that synthesized by impregnation. Such different behavior could be caused by differences in the metal particle sizes because of the reduction temperature of 1023 K

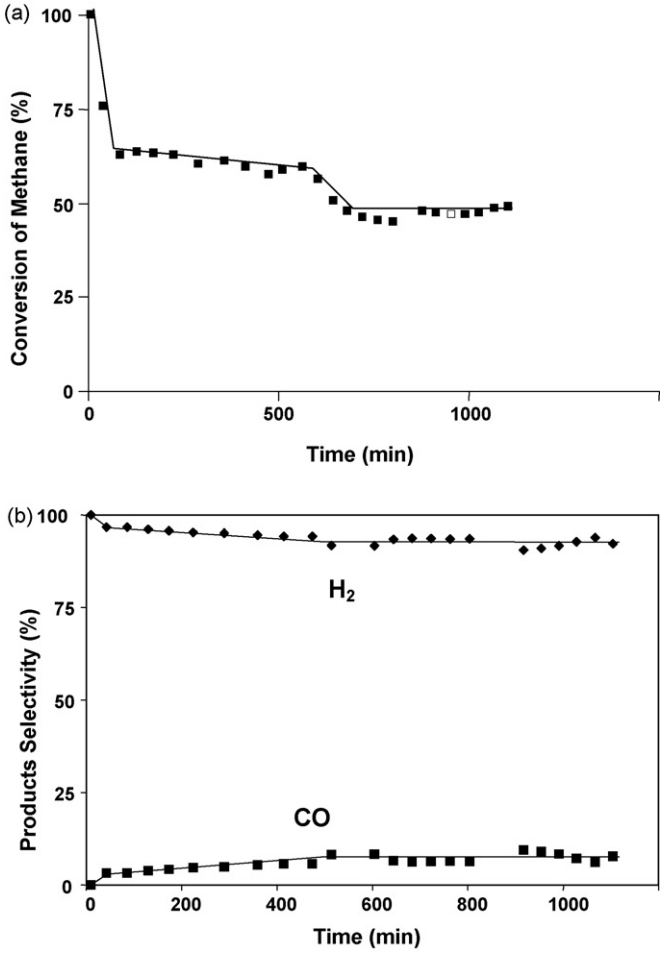

Fig. 11. Methane steam reforming on silica-supported nickel catalyst synthesized by the ammonia method performed at 973 K, atmospheric pressure and 500 h^{-1}: (a) methane conversion (%) vs. time and (b) selectivity (%) to hydrogen and carbon monoxide vs. time.

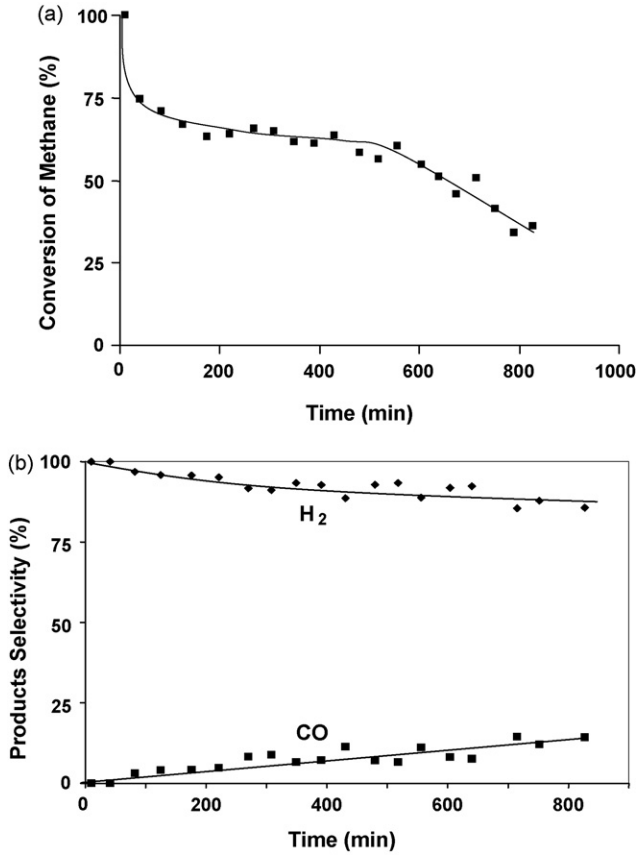

Fig. 12. Methane steam reforming on silica-supported nickel catalyst synthesized by impregnation performed at 973 K, atmospheric pressure and 500 h^{-1}: (a) methane conversion (%) vs. time and (b) selectivity (%) to hydrogen and carbon monoxide vs. time.

employed in both catalysts. The reduction temperature was just enough to collapse the high temperature metal phase observed on the silica-supported nickel catalyst. In the case of the catalyst synthesized by impregnation, such temperature was the longer superior to that required for the catalyst reduction. Therefore, the catalyst synthesized by impregnation was exposed to a high temperature for a time longer than the catalyst synthesized by the ammonia method favoring the growing of metal particle size.

4. Conclusions

Silica-supported nickel catalyst synthesized by the ammonia method and their precursors treated and not with ammonia solution were characterized by TGA, DSC, DTA thermal analysis, TPR, SEM micrographs and X-ray diffraction. Thermal decomposition kinetic parameters were calculated by the Kissinger's method.

The results indicated that the synthesized catalyst shows mainly a higher temperature metal phase (973 K), constituted by a superposition of bi-dimensional sheets similar to nickel phyllosilicate, probably resulting from the SMSI between nickel aqua ammine complex and silica surface. Such a compound degrades to stable silica-supported nickel catalyst at high temperature. Activation energies and kinetic parameters for each decomposition process were calculated by Kissinger's method. Enthalpy values were determined from differential scanning calorimetric profiles. The activity tests of such catalyst to methane steam reforming indicated that deactivation process probably caused by carbon deposition was less pronounced than deactivation of a similar nickel content catalyst prepared by impregnation.

References

[1] A. Barbier, A. Hanif, J. Dalmon, G. Martin, Appl. Catal. A: Gen. 168 (1998) 333–343.
[2] A. Loaiza-Gil, J. Arenas, M. Villarroel, F. Imbert, H. del Castillo, B. Fontal, J. Mol. Catal. A: Chem. 228 (2005) 339–344.
[3] G.A. Martin, Thesis, University Claude Bernard, Lyon (1966).
[4] G.A. Martin, B. Imelik, M. Prettre, J. Chim. Phys. 66 (1969) 1682.
[5] J.A. Dalmon, G.A. Martin, C.R. Acad. Sci. Paris 267C (1968) 1.
[6] J.A. Dalmon, G.A. Martin, B. Imelik, J. Chim. Phys. 2 (1973) 214.
[7] J.A. Dalmon, G.A. Martin, C.R. Acad. Sci. Paris 267C (1968) 610.
[8] S. Glastone, Text of Chemical Physics, second edition, Van Nostrand, New York, 1946.
[9] H.E. Kissinger, Anal. Chem. 29 (1957) 1702.
[10] E. Mikuli, A. Migdal-Mikuli, R. Chyzy, B. Grand, R. Dziembaj, Thermochim. Rec. 370 (2001) 65–71.
[11] M.A.A. Elmasry, A. Gaber, E.M.H. Khater, J. Therm. Anal. 52 (1998) 489–495.
[12] F. Bigoli, A. Braibanti, A. Tiripicchio, M. Tiripicchio Camellini, Rec. Cryst. B27 (1971) 1427.
[13] A. Malecki, R. Gajerski, S. Labus, B. Prochowska-Klisch, K.T. Wojciechowski, J. Therm. Anal. 60 (2000) 20.
[14] Z.D. Zivkovic, D.T. Zivkovic, D.B. Grujicic, J. Therm. Anal. 53 (1998) 617.
[15] R. Hyung-Seog, D. Wen-Sheng, J. Ki-Won, L. Zhomg-Wen, P. Sang-Eon, O. Young-Sam, Bull. Kor. Chem. Soc. 23 (5) (2002) 669–673.
[16] J. Li, G. Lu, Appl. Catal. A: Gen. 273 (2004) 163–170.
[17] R. Trujillano, J. Grimoult, C. Louis, J.F. Lambert, Stud. Surf. Sci. Catal. 130 B (2000).